

PSFC/JA-10-68

**Tungsten Measurement on Alcator C-Mod and EBIT  
for Future Fusion Reactors**

Podpaly, Y.A., Rice, J.E., Beiersdorfer, P.\*, Reinke, M. L.,  
Clementson, J.\*, Barnard, H.S.

\* Lawrence Livermore National Laboratory

May 2011

**Plasma Science and Fusion Center  
Massachusetts Institute of Technology  
Cambridge MA 02139 USA**

''

''

.....

''

This work was supported by the U.S. Department of Energy, Grant No. DE-FC02-99ER54512. Reproduction, translation, publication, use and disposal, in whole or in part, by or for the United States government is permitted.

# Tungsten Measurement on Alcator C-Mod and EBIT for Future Fusion Reactors

Y. A. Podpaly,<sup>1</sup> J. E. Rice,<sup>1</sup> P. Beiersdorfer,<sup>2</sup> M. L. Reinke,<sup>1</sup> J. Clementson,<sup>2</sup> and H. S. Barnard<sup>1</sup>

<sup>1</sup>*MIT Plasma Science and Fusion Center, Cambridge, MA, 02139*

<sup>2</sup>*Physics Division, Lawrence Livermore National Laboratory, Livermore, CA 94550*

Tungsten will be an important element in nearly all future fusion reactors because of its presence in plasma facing components. This makes tungsten a good candidate for a diagnostic element for ion temperature and toroidal velocity measurement, and it makes understanding tungsten emissions important for tokamak power balance. The effect of tungsten on tokamak plasmas is investigated at the Alcator C-Mod tokamak using VUV, bolometry, and soft X-ray spectroscopy. Tungsten was present in Alcator C-Mod as a plasma facing component and through laser blow off impurity injection. Quasi-continuum emission previously seen at other tokamaks has been identified. Theoretical predictions are presented of tungsten emission that could be expected in future Alcator C-Mod measurements. Furthermore, spectra of highly charged tungsten ions have been studied at the SuperEBIT electron beam ion trap. This emission could prove useful for spectroscopic diagnostics of future high-temperature fusion reactor plasmas.

## INTRODUCTION

The successful integration of fusion power plants into the power grid is expected to provide a source of clean energy in the future. Many plasma physics programs around the world are currently involved in making fusion energy production a reality. This number is expected to continue growing with the maturing of the ITER device in Cadarache, France and from the progress of the National Ignition Facility in Livermore, California. Currently, the most promising method of building a fusion power plant is the tokamak design, which uses toroidal and poloidal fields to confine the hot plasma and has so far come the closest of any magnetic fusion device to self-heated, energy producing plasma operation.

Despite the many benefits of tokamaks, there are some practical difficulties that need to be overcome. Of these the most challenging issues are the limited plasma-operation time, energy confinement, and interactions of the plasma with the walls of the tokamak vacuum vessel. Limited plasma time is caused by the poloidal field being created by a toroidal current driven in the plasma. The plasma current is driven by a central transformer which has limited flux swing and, therefore, a finite time during which it can keep the plasma confined. This problem is currently being addressed through the use of non-inductive current drive such as lower hybrid, radio-frequency current generation, [1] and the control of bootstrap current (i.e. self-generated toroidal current from pressure gradients in the plasma). The problem of plasma energy loss is two-fold: catastrophically through the contact of the plasma with the walls of the vacuum vessel and more gradually by conduction, bremsstrahlung radiation, and line emission. Bremsstrahlung radiation scales as  $T_e^{1/2}Z_{eff}$ , where  $T_e$  is the electron temperature and  $Z_{eff}$  is the effective plasma charge, defined as  $\sum n_i Z_i^2 / \sum n_i Z_i$ , so elements with high atomic number that enter the plasma increase the loss of energy through radiation. Furthermore, higher-Z elements have

more bound electrons throughout the plasma, increasing the amount of radiation lost through line emission. These losses can be extremely large and can cool down the plasma enough that it fails to maintain plasma confinement. Finally, fusion plasmas can regularly achieve temperatures in the range of millions of degrees kelvin (several keV), power fluxes on the order of 10 MW/m<sup>2</sup>, and neutron production rates exceeding 10<sup>15</sup> neutrons/s even in deuterium plasmas, and deuterium-tritium plasmas have production rates an order of magnitude higher. This places extremely stringent constraints on any material that is near the plasma; materials that have been proposed for future and current tokamaks include beryllium, carbon, molybdenum, and tungsten.

The considerations of energy balance in the plasma and plasma-material interactions come into play when choosing the material to construct the plasma wall and divertor, the location where the majority of the flux from the plasma is directed. Tungsten has recently become a material of interest in this construction because of its high melting temperature, tensile strength, and low hydrogen retention [2]. These characteristics have made it the material of choice for the ITER divertor.

Because of the likelihood of tungsten impurities entering the plasma from the wall material, tungsten has recently become an element of a great deal of interest for atomic physics. With a Z value of 74, tungsten impurities degrade plasma confinement quickly when they enter the plasma, and must remain below the level of  $2 \times 10^4 n_e$  [3]. On the other hand, the strong electron binding of tungsten allows the impurity to have bound electrons, and therefore line emission, throughout large swathes of the plasma. Efforts have already been undertaken to prepare an imaging X-ray crystal spectrometer using the expected intrinsic emission of tungsten in ITER [4].

This paper is organized as follows. In Section , Alcator C-Mod and its tungsten relevant diagnostics are introduced. In Section , tungsten measurements on Alcator C-Mod are described. Section describes the fu-

ture diagnostics planned for Alcator C-Mod. Section describes the Lawrence Livermore National Laboratory (LLNL) electron beam ion trap devices and some tungsten measurements performed using it. Section is a brief summary.

## ALCATOR C-MOD OVERVIEW

Alcator C-Mod [5] is a small high field device ( $R=0.67$ ,  $B_T = 3-8\text{T}$ ) operating in Cambridge, Massachusetts. Its toroidal magnetic fields are at the level of a fusion reactor, and its standard 5.4 T operation is in line with the proposed operating regime for ITER. Standard plasma densities are in the range of  $5 \times 10^{19} - 6 \times 10^{20} \text{ m}^{-3}$ , which is similar to predicted tokamak reactor densities. The core electron temperatures in Alcator C-Mod are generally in the 0.5-4 keV range, but higher operating regimes have been discovered that allow running up to  $T_e = 9 \text{ keV}$ . Alcator's pulse length is two seconds, but it has an energy confinement time of approximately 100 milliseconds, meaning that for most of the discharge duration (after the magnetic fields ramp-up and before the fields start to decay), the plasma is in steady-state. The times between 0.8 and 1.5 seconds into the discharge are generally usable for physics experiments. The Alcator C-Mod inner wall is constructed mostly from molybdenum tiles.

Alcator C-Mod operates in a campaign format, with several months of operation followed by weeks or months of maintenance and upgrade time. A toroidal, continuous row of tungsten tiles was installed in the Alcator divertor prior to the 2007 campaign. Over the next two campaigns, tungsten injections were not typically seen in the core plasma. After the first 2008 campaign, a row of tiles poloidally spanning the lower divertor were removed, and ion beam analysis was performed to measure tungsten redeposition. The results of this study are reported in [6]. It was found that significant amounts of tungsten had migrated throughout the divertor and coated the other tiles. No spectrometers viewing the divertor plasma were properly situated to observe tungsten emissions, but it is fair to assume that significant amounts of tungsten were present in the divertor plasma.

In early 2010, one of the divertor tungsten tiles in Alcator C-Mod was dislodged from its position and melted. After this event, plasma performance was greatly degraded, and large amounts of tungsten were seen in the plasma. By placing the strike-point, the location of the last closed flux surface on the divertor, directly on the melted tile location, it became possible to get large tungsten injections into the plasma core. These injections were large enough to disrupt plasma operation during the course of a discharge.

Also, in early 2010, a new operating regime was discovered on Alcator C-Mod in which the core electron tem-

perature reached 8 keV, which was accomplished by running at higher magnetic fields and non-standard auxiliary RF heating. This was the first time that C-Mod reached these temperatures, which allows performing ITER-like diagnostic development. A time trace of this discharge is shown in figure 1. Note that despite reaching 8 keV for the core electron temperature, the core ion temperature remains around 3 keV, which shows a very strong decoupling between those two species.

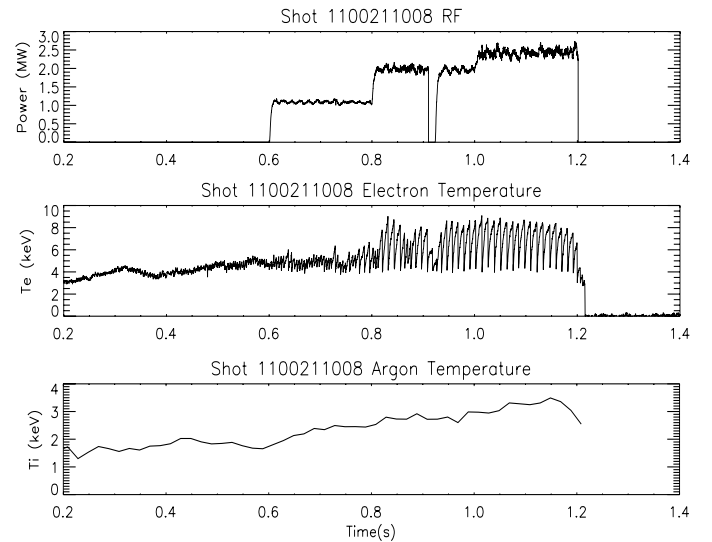


FIG. 1: Time history of an 8 keV discharge

## Diagnostics on Alcator C-Mod

C-Mod has a wide array of diagnostics for the study of plasma behavior. Generally, a bolometric system [7] is used to measure the amount of energy being emitted from the plasma in the x-ray energy band. This can confirm that an impurity has entered the plasma, but not which impurity it is. Another diagnostic commonly used on C-Mod for impurity identification is a Z-effective meter, which monitors the effective charge of the plasma through the bremsstrahlung emission.  $T_e$  and  $T_i$  measurements are performed as well through cyclotron emission measurements, Thomson scattering, and Doppler broadening of argon emission lines [8]. Argon ion temperatures at C-Mod are generally used as a proxy for the main ion temperature since the two species are assumed to be well equilibrated due to the short temperature equilibration time of highly charged argon and main plasma ions. An example time trace of a tungsten injection with its effect on radiated power and Z-effective is shown in figure 2.

In late 2009, a new grating spectrometer (XEUS) was installed on Alcator C-Mod in collaboration with LLNL to act as an impurity survey instrument [9]. This device is a novel grating spectrometer, based on instrumentation

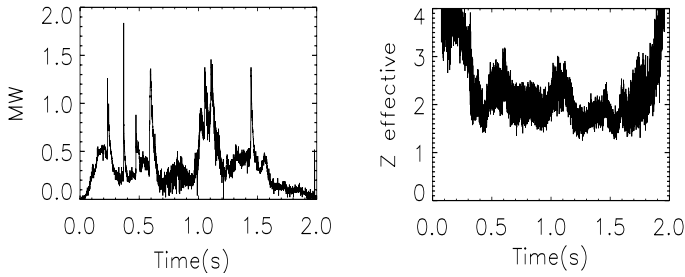


FIG. 2: Time traces of radiated power (left panel) and effective charge (right panel) of the plasma; there is a tungsten injection at approximately 1 second into the discharge which is the cause of the increase in both parameters. Other spikes are due to smaller injections from the plasma facing wall.

developed for the Livermore electron beam ion trap and NSTX spherical tokamak in Princeton [10, 11], capable of covering a large wavelength band with acceptable resolution. It ended up being the most used spectrometer for impurity emission surveys and is capable of a resolution of  $\lambda/\Delta\lambda \approx 550$  at  $50 \text{ \AA}$ .

### MEASUREMENTS ON THE ALCATOR C-MOD TOKAMAK

As was mentioned previously, over the course of the last C-Mod operational campaign, tungsten was seen in several discharges. The XEUS spectra for one of these discharges are shown in figure 3. The figure shows the temporal evolution of the  $50 \text{ \AA}$  tungsten band with colors representing various times after the start of the plasma. The emission lines noticeable before the tungsten injection are from intrinsic impurities such as carbon, oxygen, and boron and are used to calibrate the spectra. The emission lines used to calibrate the image in figure 3 are from B IV ( $1s^2 - 1s2p$ ), B IV ( $1s^2 - 1s3p$ ), B V ( $1s - 2p$ ), B V ( $1s - 3p$ ), and Ar XVI ( $1s^22s - 1s^23p$ ) with respective wavelengths of  $60.31 \text{ \AA}$ ,  $52.68 \text{ \AA}$ ,  $48.59 \text{ \AA}$ ,  $40.98 \text{ \AA}$ , and  $23.529 \text{ \AA}$ . The calibration curve is found to be  $\lambda = 80.7214 \pm 0.0480 - ch \times 0.0649 \pm 0.0001 + ch^2 \times 1.243 \times 10^{-5} \pm 9.530 \times 10^{-8}$ , where  $ch$  refers to the calibration channel. The emission lines used to calibrate the image in figure 4 are from O VIII ( $1s - 2p$ ), O VII ( $1s^2 - 1s2p$ ), B V ( $1s - 2p$ ), and C VI ( $1s - 2p$ ) with respective wavelengths  $18.97 \text{ \AA}$ ,  $21.60 \text{ \AA}$ ,  $48.59 \text{ \AA}$ , and  $33.73 \text{ \AA}$ . The calibration curve is then  $\lambda = 66.3928 \pm 0.0110 - ch \times 0.0593 \pm 3.7199 \times 10^{-5} + ch^2 \times 1.2668 \times 10^{-5} \pm 2.7277 \times 10^{-8}$ . The wavelengths for these calibrations are from [12–14]. All of these calibration elements are intrinsic impurities in the Alcator C-Mod vessel, except for argon which is added externally for diagnostic purposes.

The XEUS spectrometer has a line of sight through the C-Mod vessel which images plasma with  $T_e$  ranging from  $\sim 100 \text{ eV}$  to  $\sim 3 \text{ keV}$ . This may affect the distribu-

tion of lines since different temperatures will excite different ionization stages and energy levels, but the line identification should remain unaffected. Since the XEUS is designed to primarily act as a survey instrument, this effect is not taken into consideration in this work. It is intended, in future work, to upgrade the spectrometer with imaging capabilities to act as an impurity survey instrument with spatial resolution.

The inset in figure 3 shows a multi-line fit to the spectra performed with the IGOR Pro data analysis software. The red points are data points created by integrating over the entire tungsten injection to achieve better statistics. The IGOR Pro automatic line fitting routine was used to create this fit; user input was used only to improve, add, and subtract missing lines and poor fits. The results of this fit are shown in table I. In this table, our measurements are compared with previously published results from the Large Helical Device in Japan [15] and the TEXT tokamak [16–18]. This tungsten emission band was first identified in the PLT and ORMAK tokamaks in the 1970s [19, 20], significant work was performed on it at ASDEX [21], and it was recently identified in NSTX [22].

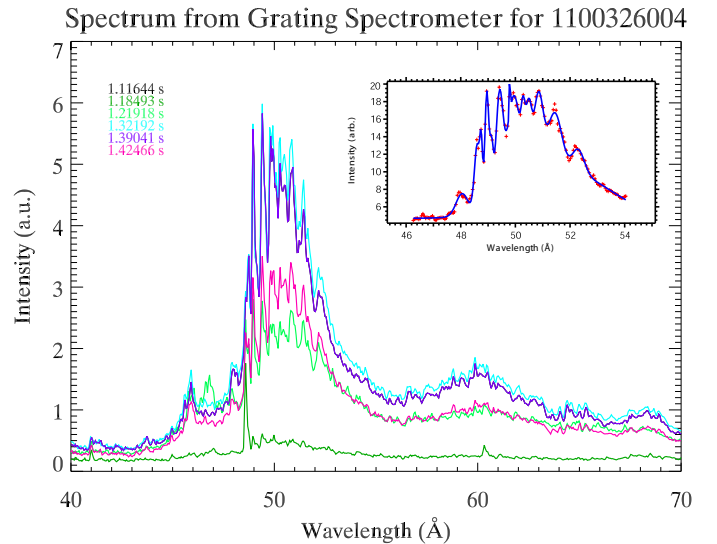


FIG. 3: Time history of tungsten injection. Colors represent different times throughout the plasma discharge. The inset shows the multi-line best fit to the data.

Later in the campaign, the XEUS spectrometer was repositioned to view lower wavelength line emission. The tungsten tiles had also been removed in order to prevent further degradation of the plasma performance. Nevertheless, tungsten was still observed in certain discharges from probes, laser blow-off impurity injection, or from possible melting of previously redeposited tungsten impurities. The  $30 \text{ \AA}$  tungsten unresolved transition array was identified and is shown in figure 4. The inset again shows the multi-line fit to the data. The results of the fit are shown in table II; however, in this case, the agreement to previously available data is worse than for the  $50 \text{ \AA}$

TABLE I: Identification of tungsten lines in the 50 Å region. Uncertainties shown are one standard deviation. <sup>a</sup> Referenced in [15]. <sup>b</sup> Referenced in [16–18]

Charge State	Measured $\lambda$ (Å)	Previously Measured $\lambda$ (Å)
W <sup>29+</sup>	49.94 ± .01	49.99 ± .03 <sup>a</sup> , 49.938 ± .005 <sup>b</sup>
W <sup>29+</sup>	49.79 ± .09	49.856 ± .005 <sup>b</sup>
W <sup>28+</sup>	49.00 ± .01	49.00 ± .02 <sup>a</sup> , 48.948 ± .005 <sup>b</sup>
W <sup>27+</sup>	52.30 ± .03	52.31 ± .03 <sup>a</sup>
W <sup>27+</sup>	51.43 ± .02	51.42 ± .02 <sup>a</sup> , 51.457 ± .005 <sup>b</sup>
W <sup>27+</sup>	50.84 ± .02	50.87 ± .02 <sup>a</sup>
W <sup>27+</sup>	49.41 ± .01	49.44 ± .02 <sup>a</sup>
W <sup>27+</sup>	48.05 ± .03	48.02 ± .02 <sup>a</sup>
W <sup>27+</sup>	48.75 ± .01	48.729 ± .005 <sup>b</sup>
Unid.	48.61 ± .02	
Unid.	49.13 ± .01	
Unid.	50.28 ± .02	

Å region. This decreased agreement is likely due to the resolution of the spectrometer being unable to separate the numerous lines in the transition array.

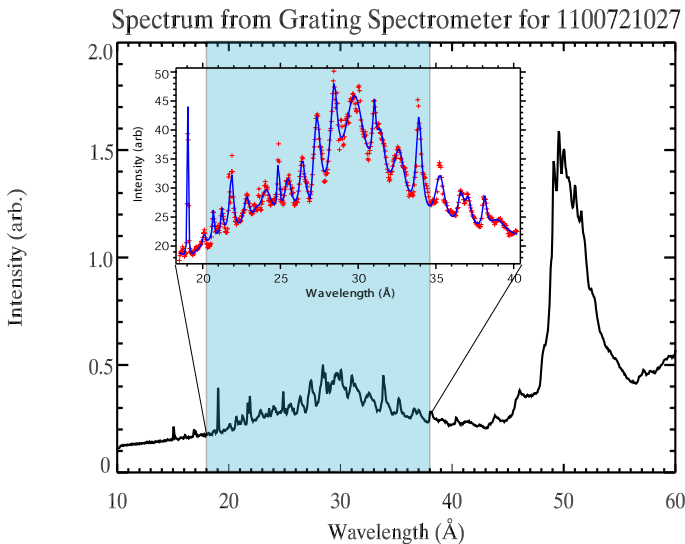


FIG. 4: Tungsten emission from the 30 Å unresolved transition array, which is highlighted. The 50 Å region is shown as well but is out of focus in this setup and is not usable. The inset shows the multi-line best fit to the data.

### MODELING AND FUTURE WORK ON ALCATOR C-MOD

With these measured tungsten data, Alcator C-Mod has joined in the effort to study tungsten plasma impurities. In the future, it will be possible to study higher energy transitions and impurity behavior at reactor-like electron densities and near reactor-like temperatures.

TABLE II: Identification of tungsten lines in the 30 Å unresolved transition array. Identifications are approximate and are matched up as closely as feasible to previously published results. Uncertainties shown are one standard deviation. All previously measured wavelengths are from [15].

Charge State	Measured $\lambda$ (Å)	Previously Measured $\lambda$ (Å)
Unid.	20.69 ± .01	
Unid.	20.88 ± .02	
Unid.	22.84 ± .02	
Unid.	23.43 ± .09	
Unid.	24.08 ± .05	
Unid.	24.87 ± .01	
Unid.	25.49 ± .02	25.36 ± .02
Unid.	26.41 ± .01	
Unid.	26.93 ± .03	26.87 ± .04
Unid.	27.35 ± .01	
Unid.	28.45 ± .01	28.32 ± .05
Unid.	28.45 ± .01	28.32 ± .05
Unid.	29.77 ± .02	29.51 ± .03
W <sup>25+</sup>	31.03 ± .01	30.90 ± .03
Unid.	31.45 ± .03	
W <sup>24+</sup>	32.63 ± .02	32.50 ± .05
W <sup>22+?</sup>	35.26 ± .02	35.86 ± .07
W <sup>22+?</sup>	36.60 ± .04	35.86 ± .07
Unid.	37.08 ± .04	
W <sup>21+</sup>	38.14 ± .02	38.13 ± .07
Unid.	38.97 ± .13	

Two spectrometers are currently in the development stages to take advantage of this opportunity.

The first is a one-channel cylindrically bent crystal spectrometer. The system is tangentially viewing and is designed to look at the 3-4 Ni-like emission line around 5.68 Å with approximately 100 mÅ coverage. Using the HULLAC [23] code and approximate fractional abundances from [24], it is possible to predict the expected spectrum to be seen by this spectrometer for standard C-Mod plasmas (shown in figure 5). For higher electron temperatures, there is expected to be more Ni-like atoms than the other ionization stages and, thus, higher intensity in that line.

The second planned device is an imaging X-ray crystal spectrometer based on the system currently in use on Alcator C-Mod for ion and velocity profile measurements [25]. This system will act as a prototype for the planned ITER core imaging spectrometer, and is intended to measure emissions from the lower charge states of the same transitions. Predicted spectra of the hot C-Mod plasma using the Flexible Atomic Code (FAC) [26] with Doppler broadening were created. The modeling uses the same methodology as the ITER predicted spectral modeling from [4]. One of these predicted spectra for 8 keV electrons and 2 keV ions is shown in figure 6.

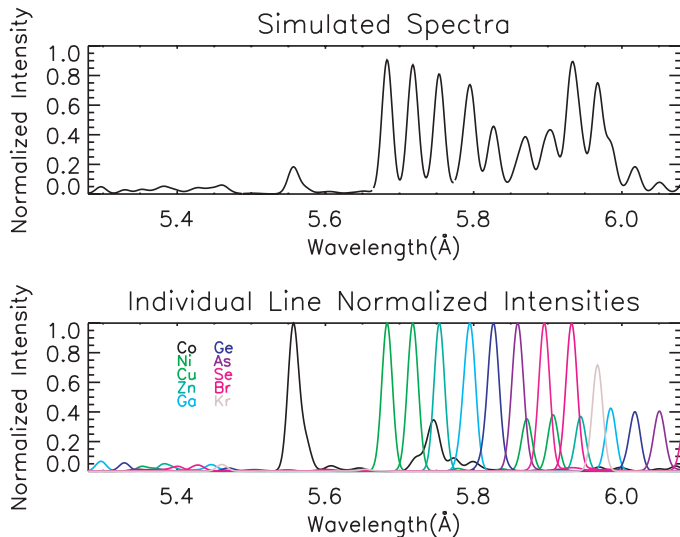


FIG. 5: HULLAC predictions for tungsten emissions near 5.7 Å with  $T_e \approx 3$  keV.

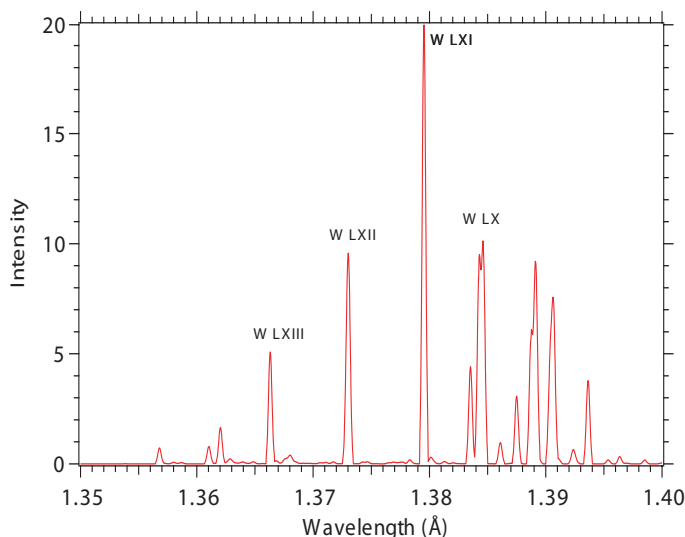


FIG. 6: FAC modeling of C-Mod discharge with 8 keV electron temperature and 2 keV ion temperature.

Both of these spectrometers will allow a better understanding of impurity transport on C-Mod and of the suitability of tungsten as a diagnostic element. In particular, the imaging spectrometer will be useful as a prototype for the ITER imaging system and will be able to quantify the usefulness of intrinsic tungsten for temperature and velocity measurements.

## LAWRENCE LIVERMORE NATIONAL LABORATORY EBIT

Alcator C-Mod is a good machine for the study of impurity transport and for investigations of atomic spectra

at high density and moderate temperatures. Due to large numbers of ion species and spectrometer line-of-sight integrations over plasma regions with varying density and temperature, the tokamak is not always ideal for atomic physics studies. Spectroscopic measurements under controlled plasma conditions are preferably performed on electron beam ion traps (EBIT), where a tunable electron beam ionizes, excites, and confines a small volume of ions [27].

At LLNL, two EBIT devices are in operation: EBIT-1 and SuperEBIT [28]. These have been employed for several spectroscopic measurements of tungsten (see Clementson et al. in this volume). The controlled plasma conditions and the excitation energies available at the LLNL EBITs allow the study of tungsten spectra that cannot easily be measured with other laboratory plasma sources. For present-day tokamaks, the EBITs also offer unique opportunities for experimental investigations. For instance, in the work by Clementson et al. [29], the range of electron temperatures in Alcator C-Mod for the Ni-like tungsten lines was studied, and there is good agreement between the HULLAC modeling performed and the measured spectra. Another example is the measurement of the  $2s_{1/2}-2p_{3/2}$  transitions in F-like  $W^{65+}$  through Li-like  $W^{71+}$  using SuperEBIT operated at an electron-beam energy of 103 keV [30]. Figure 7 displays lines from all the tungsten charge states with an incompletely filled L-shell, measured in the latter work with a flat-crystal spectrometer.

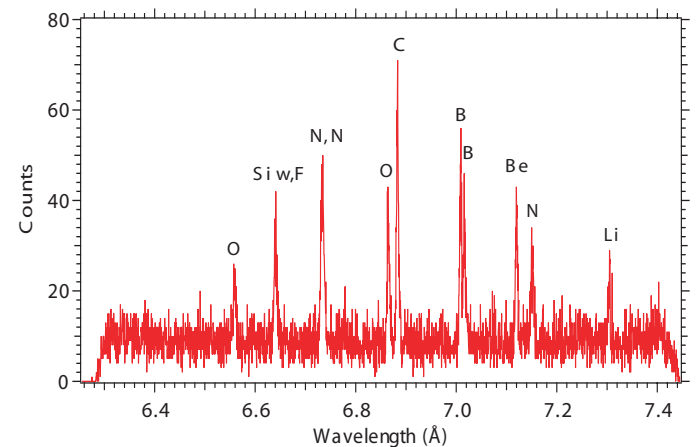


FIG. 7: Measurement of the  $2s_{1/2}-2p_{3/2}$  lines in Li-like through F-like tungsten. The labels refer to the charge state forming the line. The “Si w” label refers to the  $1s_{1/2}-2p_{3/2}$  resonance line from a silicon impurity in the EBIT chamber.

## DISCUSSION

Tungsten has been observed on Alcator C-Mod using the XEUS grating spectrometer. Tungsten impurity ions

have been noticed to have a detrimental effect on tokamak plasma operations. Nevertheless, the Alcator C-Mod spectroscopic observations of the tungsten quasi-continuum around 50 Å and 30 Å have added to the data from previous EUV measurements of tungsten at the ORMAK, PLT, TEXT, ASDEX Upgrade, LHD, and NSTX devices. The diagnostic set-up allows the comparison of the tungsten line identifications with previous measurements, and agreement in the better resolved 50 Å region is within experimental error for a large fraction of the lines to the LHD results. In the future, Alcator C-Mod intends to take part in diagnostic development for the ITER X-ray crystal spectrometer, notably by performing atomic physics measurements in near ITER-like plasma parameters.

Until ITER or similar fusion reactors are operational, the best way to perform fusion relevant atomic physics measurements are EBIT like devices. The LLNL EBIT, in particular, has performed a large amount of research on tungsten in various energy ranges that are applicable to fusion research.

#### ACKNOWLEDGMENTS

The authors would like to thank M. F. Gu, G. V. Brown, E. W. Magee, A. Bader, C. Gao, L. Delgado-Aparicio, M. Bitter, K. Hill, and E. Marmor for their help with this work. This work was supported by Fusion Energy Sciences Program, administered by Oak Ridge Institute for Science and Education under a contract between the U.S. Department of Energy and the Oak Ridge Associated Universities, the Department of Energy under Contract No. DE-AC52-07NA-27344 and the Laboratory Directed Research and Development program under Project No. 09-ERD-016, and the Department of Energy under Contract No. DE-FC02-99ER54512.

- 
- [1] N. J. Fisch. *Rev. Mod. Phys.*, 59(1):175–234, Jan 1987.
- [2] B. Lipschultz, J. Roth, J. W. Davis, R. P. Doerner, A. A. Haasz, A. Kalenbach, A. Kirschner, R. D. Kolasinski, A. Loarte, V. Philipps, K. Schmid, W. R. Wampler, G. M. Wright, and D. G. Whyte. *MIT Plasma Science and Fusion Center Report*, RR-10-4, 2010.
- [3] R. Neu. *Phys. Scripta*, 2006(T123):33, 2006.
- [4] P. Beiersdorfer, J. Clementson, J. Dunn, M. F. Gu, K. Morris, Y. Podpaly, E. Wang, M. Bitter, R. Feder, K. W. Hill, D. Johnson, and R. Barnsley. *J. Phys. B.*, 43(14):144008, 2010.
- [5] Alcator C-Mod Team. *Fus. Sci. Tech.*, 51(3), 2007.
- [6] H. S. Barnard, D. G. Whyte, and B. Lipschultz. *J. Nucl. Mater.*, In Press, 2010.
- [7] M. L. Reinke and I. H. Hutchinson. *Rev. Sci. Instrum.*, 79(10):10F306, 2008.
- [8] I. H. Hutchinson. *Principles of Plasma Diagnostics*. Cambridge University Press, 2002.
- [9] M. L. Reinke, P. Beiersdorfer, N. T. Howard, E. W. Magee, Y. Podpaly, J. E. Rice, and J. L. Terry. *Rev. Sci. Instrum.*, 81:10D736, 2010.
- [10] P. Beiersdorfer, M. Bitter, L. Roquemore, J. K. Lepson, and M.-F. Cu. *Rev. Sci. Instrum.*, 77(10):10F306, 2006.
- [11] P. Beiersdorfer, J. K. Lepson, M. Bitter, K. W. Hill, and L. Roquemore. *Rev. Sci. Instrum.*, 79(10):10E318, 2008.
- [12] Yu. Ralchenko, A.E. Kramida, J. Reader, and NIST ASD Team. *NIST Atomic Spectra Database*. Available: <http://physics.nist.gov/asd>
- [13] J. K. Lepson, P. Beiersdorfer, E. Behar, and S. M. Kahn. *Astrophys. J.*, 590:604617, 2003.
- [14] R. L. Kelly. *J. Phys. Chem. Ref. Data*, Supplement 1, 1987.
- [15] M. B. Chowdhuri, S. Morita, M. Goto, H. Nishimura, K. Nagai, and S. Fujioka. *Plasma Fusion Res.*, 2:S1060, 2007.
- [16] J. Sugar, V. Kaufman, and W. L. Rowan. *J. Opt. Soc. Am. B*, 10(8):1321–1325, 1993.
- [17] J. Sugar, V. Kaufman, and W. L. Rowan. *J. Opt. Soc. Am. B*, 10(11):1977–1979, 1993.
- [18] J. Sugar, V. Kaufman, and W. L. Rowan. *J. Opt. Soc. Am. B*, 10(5):799–801, 1993.
- [19] E. Hinnov and M. Mattioli. *Phys. Lett. A*, 66(2):109 – 111, 1978.
- [20] B. M. Johnson, K. W. Jones, J. L. Cecchi, E. Hinnov, and T. H. Kruse. *Phys. Lett. A*, 70(4):320 – 322, 1979.
- [21] T. Pütterich, R. Neu, R. Dux, A. D. Whiteford, M.G. O’Mullane, and the ASDEX Upgrade Team. *Plasma Physics Control. F.*, 50(8):085016, 2008.
- [22] J. Clementson, P. Beiersdorfer, A. L. Roquemore, C. H. Skinner, D. K. Mansfield, K. Hartzfield, and J. K. Lepson. *Rev. Sci. Instrum*, 81:10E326, 2010.
- [23] A. Bar-Shalom, M. Klapisch and J. Oreg. *J. Quant. Spectrosc. Rad. Transfer.*, 71(2-6):169–188, 2001.
- [24] J. Yanagibayashi, T. Nakano, A. Iwamae, H. Kubo, M. Hasuo, and K. Itami. *Nucl. Instrum. Meth. A*, 623:2, 2010.
- [25] A. Ince-Cushman, J. E. Rice, M. Bitter, M. L. Reinke, K. W. Hill, M. F. Gu, E. Eikenberry, Ch. Broennimann, S. Scott, Y. Podpaly, S. G. Lee, and E. S. Marmor. *Rev. Sci. Instrum.*, 79(10):10E302, 2008.
- [26] M. F. Gu. *Can. J. Phys.*, 86:675–689, June 2008.
- [27] M. A. Levine, R. E. Marrs, J. N. Bardsley, P. Beiersdorfer, C. L. Bennett, M. H. Chen, T. Cowan, D. Dietrich, J. R. Henderson, D. A. Knapp, A. Osterheld, B. M. Penetrante, M. B. Schneider, and J. H. Scofield. *Nucl. Instrum. Methods*, B43:431–440, 1989.
- [28] P. Beiersdorfer. *Can. J. Phys.* 86(1):1–10, 2008.
- [29] J. Clementson, P. Beiersdorfer, G. V. Brown, and M. F. Gu. *Phys. Scripta*, 81(1):015301, 2010.
- [30] Y. Podpaly, J. Clementson, P. Beiersdorfer, J. Williamson, G. V. Brown, and M. F. Gu. *Phys. Rev. A*, 80(5):052504, 2009.